PFC/JA-96-18

# Local Impurity Puffing as a Scrape-off Layer Diagnostic on the Alcator C-Mod Tokamak

D. Jablonski, B. LaBombard, G.M. McCracken, S. Lisgo[1],
B. Lipschultz, I.H. Hutchinson, J. Terry, P.C. Stangeby[1]

June 1996

[1]Institute of Aerospace Studies, University of Toronto, Ont. M3H 5T6, Canada.

Submitted to Jour. of Nuclear Materials.

This work was supported by the U. S. Department of Energy Contract No. DE-AC02-78ET51013. Reproduction, translation, publication, use and disposal, in whole or in part by or for the United States government is permitted.

# Local Impurity Puffing as a Scrape-off Layer Diagnostic on the Alcator C-Mod Tokamak

D. Jablonski, **B. LaBombard**, G.M. McCracken, S. Lisgo,*
B. Lipschultz, I.H. Hutchinson, J. Terry, and P.C. Stangeby.*

Plasma Fusion Center
Massachusetts Institute of Technology
Cambridge, MA 02139, USA.

**Abstract**

A capillary injection system has been installed on Alcator C-Mod which allows the localized introduction of gaseous species at a variety of poloidal locations. An experimental programme has been undertaken to observe impurity puffs with a CCD camera through appropriate optical filters. The comet-like shape of an ion line emission plume formed in the region of an injection graphically displays the direction of background Deuterium flow as well as that of the poloidal impurity ion drift. Parallel and cross-field one-dimensional fluid models are used to characterize the plume shapes and extract the background plasma temperature and parallel flow velocity and the impurity ion poloidal drift. Model results are benchmarked against simulations of DIVIMP, a Monte Carlo code, and fast scanning probe measurements. In addition to elucidating local edge impurity transport, the experiments present a novel diagnostic technique.

## 1. Introduction

Observing the line emission patterns formed in the region of the scrape-off layer of an impurity puff provides unique opportunities for investigation of impurity transport as well as diagnosis of the background plasma. The experiments on Alcator C-Mod [1] have involved imaging plumes at a range of poloidal locations in a variety of plasma discharges, with both lower and upper x-points, in normal and reversed field configurations. This paper discusses general observations, focusing on analysis of the first charge state plumes formed at the inner-wall midplane viewed from the outboard.

Such plumes have been observed and modeled on other machines. Two methods of modeling these emission patterns have been employed: the use of a complex fluid or Monte Carlo code, as was done by Matthews [2], McCracken [3], and Pitcher [4], and the use of simple analytic coulomb collision and ionization relations, as was done by Pitcher

* University of Toronto IAS, Toronto M3H 5T6, Canada.

[5]. An intermediate approach has been taken in this work, namely using fluid models which are more complete than the simple analytic relations, but simple and straightforward enough for ease in implementation and interpretation. A benefit of this method is the potential to analyze a large number of images in relatively short order, allowing the technique to be used as a regular diagnostic. The efficacy of this fluid paradigm is evaluated by comparison with calculations of DIVIMP [6,7], a Monte Carlo code, and with measurements of the C-Mod fast scanning probe [8,9]. It should be noted that while the proposed methodology was different, plasma parameter extraction from impurity plume shapes has been previously discussed by Stangeby and Elder [10].

## 2. Experiments

The primary tools for the experiments are shown in figure 1. The Neutral gas INJection Array (NINJA) is a capillary puffing system which can deliver gaseous species at 20 poloidal and 5 toroidal locations [11]. Puff locations discussed below are labeled A, B, and C for reference. Line emission patterns produced in the vicinity of the puffs are imaged with CCD cameras through selectable optical filters with the two views marked on the figure. The cameras are located outside the vessel, with coherent fiber bundles leading to a standard C-mount lens at the view. The cameras are controlled with Multiple Automatic Camera Exposure Control and Display (MACECAD) units [12]. Profile measurements of density, electron temperature, floating potential, and parallel flow in the SOL are provided by the fast scanning probe at the poloidal location shown in the figure. All of the discussed experiments were performed in 800 kAmp, 5.3 Tesla on axis, single-null diverted discharges.

The shape of the ion plumes observed is typically comet-like, with a tail extending along the field line towards the nearest strike-point. An example of this is shown in figure 2. For this lower x-point shot, Nitrogen was puffed simultaneously at the inner and outer divertors (locations B and C) while viewed with the top camera through an N-II filter. The tail of each plume is directed towards the appropriate strike-point, CCW viewed from the top at the outer divertor and CW at the inner. This behaviour is observed through both -II and -III filters, regardless of $\underline{\mathbf{B}}\times\nabla B$ drift direction, x-point location, or other discharge parameters. Figure 3 shows contour plots of C-II plumes during methane puffs at the inner midplane (location A) observed with the side camera in upper and lower x-point shots. In both cases, the parallel flow is directed towards the appropriate strike point.

Work has focused on the inner-wall midplane because of the excellent view accorded by the side camera, and because the geometry and transport can be easily unfolded. Neutral emission (observed for He-I during Helium injection) is seen to be

circular in shape, approximately Gaussian in profile with a FWHM of 3.5 cm about the injection site. The ion profiles, as mentioned above, are asymmetric. This asymmetry is attributed to coulomb collisions with flowing background Deuterium. One might posit other explanations, such as a local radiative cooling effect, but such hypotheses are disproved by the observation that a plume shape does not alter with a change in gas injection rate. While the emission profile shapes are obviously dominated by parallel transport of the ions (competing with ionization to the next charge state), evidence of perpendicular transport is seen as well. In shots with a downward $\underline{\mathbf{B}}\times\nabla B$ ion drift direction, the plumes are seen to have upward deviations from the field line, indicating poloidally upward impurity ion drift.

## 3. Model

Two-dimensional plumes are integrated across and along the field line to obtain parallel and perpendicular profiles respectively. These profiles are modeled with the fluid equations discussed below. While the impurity ions lack self-collisionality, the high collisionality these ions have with the background Deuterium lends validity to the application of local fluid parameters [11]. Analysis is restricted to the first charge state of the impurities.

The parallel transport of the ions is characterized with a set of continuity, momentum, and energy equations (where x is the parallel spatial variable):

$$\frac{d}{dx}(nv) = S_n - nn_e < \sigma v >_i \tag{1}$$

$$\frac{d}{dx}(nv^2 + \frac{nT}{m}) = n\frac{v_D - v}{\tau_v} - nvn_e < \sigma v >_i \tag{2}$$

$$\frac{d}{dx}(\frac{1}{2}nv^3 + \frac{5}{2}\frac{nT}{m}v) = n\frac{T_D - T}{\tau_T} + nv\frac{v_D - v}{\tau_v} - (\frac{1}{2}nv^2 + \frac{3}{2}\frac{nT}{m})n_e < \sigma v >_i \tag{3}$$

for which unscripted variables represent impurity ion parameters, $n_e$ the background electron density, $T_D$ and $v_D$ the background Deuterium temperature and parallel velocity, and the rate coefficients the ionization to the next charge state. The appropriate coefficients given by Bell [13] are used. The particle source term, $S_n$, constitutes ionization from the neutral state. Its shape is taken as that of the observed neutral emission profiles (Gaussian, FWHM of 3.5 cm). The characteristic momentum ($\tau_v$) and energy ($\tau_T$) equilibration times given by Spitzer [14] are employed to account for coulomb collisions with the background plasma. The background plasma values are taken as constant. Three inputs are needed ($n_e$, $T_D$, and $v_D$) to solve the equations for the three outputs (profiles of impurity ion n, T, and

v). To match an experimentally observed profile with a modeled density profile, n, the electron density, $n_e$, is taken as given (provided by scanning probe measurements), and the background plasma temperature and Deuterium ion velocity are found which provide the best fit.

The perpendicular behaviour of the ions is characterized with a continuity equation (where z is the spatial variable):

$$-D\frac{d^2n}{dz^2} + v\frac{dn}{dz} + n_e < \sigma v >_i n = S_o e^{-(z/\lambda)^2} \qquad (4)$$

where D and v are the poloidal diffusion coefficient and drift velocity respectively. The Gaussian form of the particle source has been inserted (with $\lambda = 2$ cm). Assuming D and v are constant, this equation can be solved analytically in terms of error functions. Because the characteristic diffusion lengths are much smaller than the width of the source, the solutions are insensitive to the value of D employed. To match a given perpendicular profile, the density (provided by the scanning probe or other means), temperature (found with the parallel solution), and diffusion coefficient are taken as given, and the value of poloidal drift velocity which provides the best fit is found. In summary, for a given two-dimensional plume and specified background electron density, equations 1-4 are used in tandem to find the background temperature, the background Deuterium parallel velocity, and the impurity ion poloidal drift.

DIVIMP (DIVertor IMPurities), a three dimensional edge impurity transport Monte Carlo code, is used to benchmark the model. DIVIMP accounts for phenomena not covered by the fluid equations, namely partial collisionality and three-dimensional aspects of impurity transport. Further, the comparison provides a check against a code with a proven track record. The results of one such comparison are shown in figure 4. For this case, typical edge density and temperature radial profiles, a parallel Deuterium velocity of 13000 m/sec, and a poloidal impurity ion drift of 1500 m/sec are modeled to produce a plume which is integrated to obtain the parallel and perpendicular profiles. Using the plasma density at the radial location where DIVIMP gives the C-II density as peaked ($n_e$ of $2.3 \times 10^{19} m^{-3}$), the best fluid model fits are shown in the figure. The resultant temperature, 16.2 eV, compares with 17 eV at the radial location where C-II is peaked. The fluid model found velocity values of 12400 and 1800 m/sec are within 5 and 15% of the DIVIMP modeled values respectively.

## 4. Results

An example of the fluid analysis for an experimental plume is shown in figure 5. This plume was observed in a lower x-point discharge with a core volume averaged

electron density ($\bar{n}_e$) of $2.1 \times 10^{20} m^{-3}$. The electron density measured by the scanning probe at the appropriate flux surface is employed ($5.6 \times 10^{19} m^{-3}$). While the scanning probe and plume are at different poloidal locations (see figure 1), one expects plasma pressure outside of the divertor region to be conserved along a field line, meaning that if the plume derived temperature matches that measured by the scanning probe, the accuracy of the density used by the model for the inner-wall puff location is verified. The temperature found with the parallel solution, 10.2 eV, does show agreement with that of the scanning probe (9.5 eV). A parallel Deuterium Mach number of .4 (towards the lower divertor) and a poloidal impurity ion drift of 365 m/sec (upward) are found. If this drift is due to $\underline{\mathbf{E}} \times \underline{\mathbf{B}}$, it would correspond to a radially outward electric field of 2920 V/m.

Error analysis shows the uncertainty of resultant temperature and poloidal drift to be relatively small. Uncertainty in the temperature, primarily due to possible error in the employed density, is 10% or less, and uncertainty in the drift velocity, primarily due to uncertainty in the ionization rate coefficients used by the model, is on the order of 20%. For Mach number, the accuracy of the assumed density is critical. Roughly speaking, the Mach number will be known only as well as is the electron density at the plume location. If the uncertainty of that density is 20%, the error bar on the Mach number will be about 20% as well.

Parameters derived from plume analysis for one C-Mod run are compared with scanning probe measurements in table 1. All of the shots had lower x-points. The values of $\bar{n}_e$, along with the measurements of temperature, Mach number, and electric field are listed. Fast scanning probe Mach numbers are derived from the ratio of upstream to downstream ion saturation current with the Hutchinson formulation, which sets momentum and particle diffusivities equal in its derivation of the appropriate fluid equations [15]. Radial electric fields at the scanning probe are calculated by taking the derivative of the plasma potential found with standard Langmuir probe theory.

While the temperature comparison in the table is a quantitative one, the Mach number and electric field comparisons should be viewed qualitatively. Excellent temperature agreement is shown in the third and fourth columns, validating the model use of the scanning probe measured electron density. The scanning probe measurements of Mach number indicate the order of magnitude of flow velocity one would expect in the C-Mod SOL outside the divertor region. Mach numbers obtained from both the plumes and the probe range between .1 and .5. The negative values for the scanning probe measurements indicate flow towards the outer strike point (as opposed to the flow towards the inner strike-point indicated at the inner-wall). Electric field values on the order of $10^3$ are seen by both measures. The observation that plume and scanning probe measured

electric field are often much different is not surprising, both because different values are expected at the two locations, and because the uncertainty of the calculated electric field at the scanning probe is about 50%.

## 5. Conclusions

These experiments have demonstrated that plumes can play a unique role in diagnosing the C-Mod edge layer. The direction of flow of the background Deuterium ions and the direction of the impurity ion drift are clearly seen in the raw experimental data. This on its own is of value because of the great flexibility and ease of use of the technique. Plumes can be observed wherever a capillary puff location with a view available of it is located. A relatively simple fluid model can be used to determine the background temperature, parallel flow velocity, and impurity ion poloidal drift. The model paradigm has been shown valid through quantitative comparison with DIVIMP and scanning probe measured temperature, and qualitative comparison with scanning probe measures of Mach number and electric field. With a more complete system, density and other parameters could in principle be extracted with this technique. However, as the plumes are now viewed and modeled on C-Mod, a reliable independent measure of density is required for analysis.

## Acknowledgments

The authors would like to express their gratitude to Bob Childs and Tom Toland for their work in construction and implementation of NINJA, to Aaron Allen for constructing the PC based system which digitizes and archives the plume images, and to the other scientists, engineers, technicians, students, and support staff of the Alcator C-Mod team whose dedicated efforts have made this work possible. This work is supported by the U.S. Department of Energy under contract No. DE-AC02-78ET5103.

## References

[1] I.H. Hutchinson, R. Boivin, F. Bombarda, et al, Phys. Plasmas 1 (1994) 1511.

[2] G.F. Matthews, D.N. Buchenauer, D.N. Hill, et al, 18th European Conference on Controlled Fusion and Plasma Physics (1990), III-229.

[3] G.M. McCracken, U. Samm, S.J. Fielding, et al, J. Nucl. Mater. 176-177 (1990) 191.

[4] C.S. Pitcher, P.C. Stangeby, D.H.J. Goodall, et al, J. Nucl. Mater. 162-164 (1989) 337.

[5] C.S. Pitcher, PhD Thesis, University of Toronto IAS (1987).

[6] P.C. Stangeby, C. Farrell, S. Hoskins, et al, Nuclear Fusion 28 (1988) 1945.

[7] P.C. Stangeby and J.D. Elder, J. Nucl. Mater. 196-198 (1992) 258.
[8] B. LaBombard, J. Goetz, C. Kurz, et al, Phys. Plasmas 2 (1995) 2242.
[9] B. LaBombard, J. Goetz, I.H. Hutchinson, et al, these proceedings.
[10] P.C. Stangeby and J.D. Elder, Plasma Phys. Control. Fusion 33 (1991) 1435.
[11] D. Jablonski, PhD Thesis, MIT Plasma Fusion Center (1996).
[12] D.H.J. Goodall and M.N. Price, J. Nucl Mater. 196-198 (1992) 1047.
[13] K.L. Bell, H.B. Gilbody, J.G. Hughes, et al, Atomic and Molecular Data for Fusion, Part I, UKAEA Report CLM-R216 (1982).
[14] L. Spitzer, Jr., Physics of Fully Ionized Gases (Interscience, New York, 1956).
[15] I.H. Hutchinson, Phys. Fluids 30 (1987) 3777.

*Fig. 1 - Layout of plume experiments on the Alcator C-Mod tokamak: the capillary puff locations utilized in the experiments discussed are marked with arrows and labeled for reference; eyes indicate the CCD camera views; the fast scanning probe poloidal location and trajectory are shown.*

*Fig. 2 - Top camera view through N-II filter of simultaneous Nitrogen puffs at inner and outer divertor (locations B and C). The tail of each plume extends along the field line towards the appropriate strike-point.*

*Fig. 3 - Contour plots of images of methane puffs at inner-wall midplane (location A) viewed by side camera through a C-II filter in lower and upper x-point discharges; background Deuterium ion flow is indicated towards the appropriate strike-point in both shots.*

*Fig. 4 - Best fluid model fits to integrated parallel and perpendicular profiles of C-II plume produced by DIVIMP. DIVIMP utilizes typical C-Mod edge profiles of density and temperature. Using the electron density at the radial location where DIVIMP has C-II ions peaked, the fluid model fits a temperature of 16.2 eV (compared with 17 eV at the flux surface of the employed density), a parallel Deuterium flow velocity of 12,400 m/sec (13,000 input to DIVIMP), and an impurity ion drift of 1800 m/sec (1500 input to DIVIMP).*

*Fig. 5 - Best fluid model fits to integrated profiles of an inner-wall midplane (location A) N-II plume viewed by the side camera. Using the electron density measured by the scanning probe at the appropriate flux surface, the model fits to a temperature of 10.2 eV (compared with 9.5 eV measured by the scanning probe), a Mach number of .4, and a poloidal impurity ion drift of 365 m/sec.*

*Table 1 - Plume and fast scanning probe measurement comparison for shots of one run. While temperature comparison should be viewed quantitatively, comparisons of Mach number and radial electric field are meant to be qualitative (since measurements are made at different poloidal locations).*

| **Core $n_e$** | | **Temperature (eV)** | | **Mach Number** | | **$E_r$-Field (V/m)** | |
|---|---|---|---|---|---|---|---|
| **$x10^{20} m^{-3}$** | **Species** | **Plume** | **FSP** | **Plume** | **FSP** | **Plume** | **FSP** |
| 1.5 | N-II | 7.5 | 8.0 | .20 | -.44 | 1360 | 1100 |
| 2.1 | N-II | 10.0 | 9.5 | .35 | -.32 | 2190 | 1900 |
| 2.1 | N-II | 10.0 | 9.5 | .40 | -.36 | 2920 | 1500 |
| 2.3 | He-II | 17.0 | 15.5 | .15 | -.20 | 1080 | 3700 |
| 1.7 | He-II | 20.0 | 20.5 | .25 | -.14 | 420 | 5000 |
| 1.2 | N-II | 8.0 | 8.0 | .25 | -.36 | 520 | 1500 |

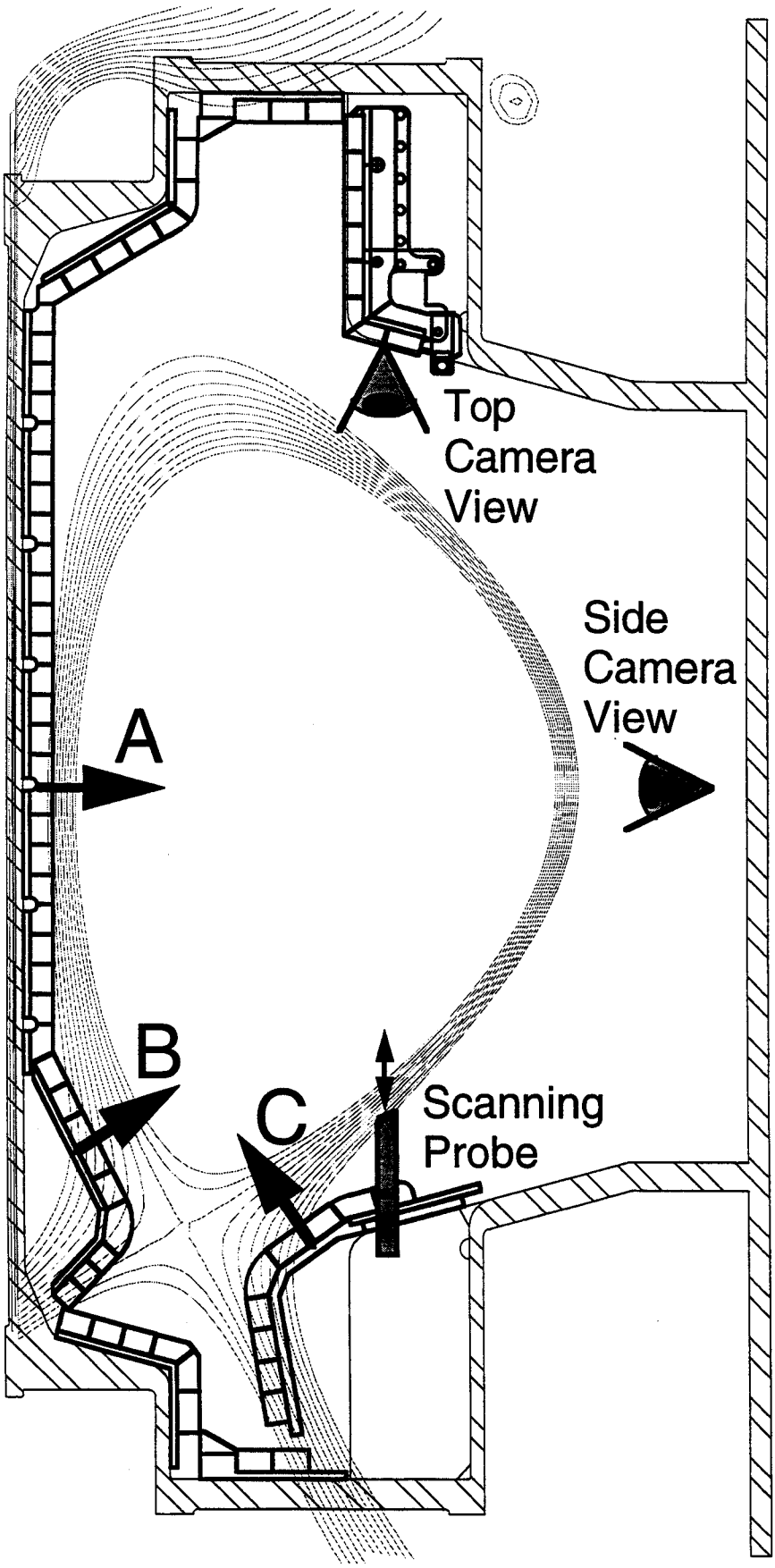


Figure 1

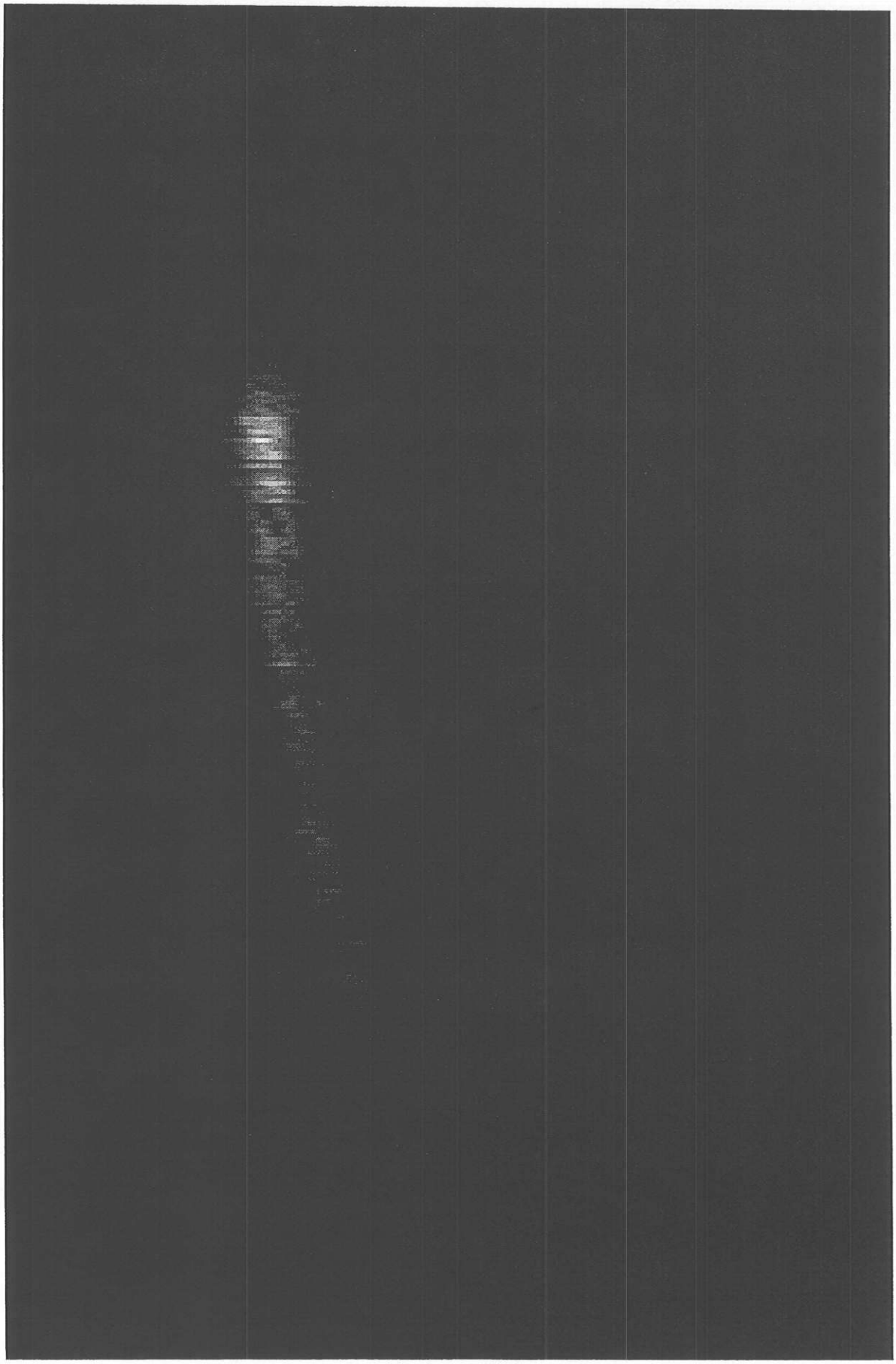

Figure 2
10

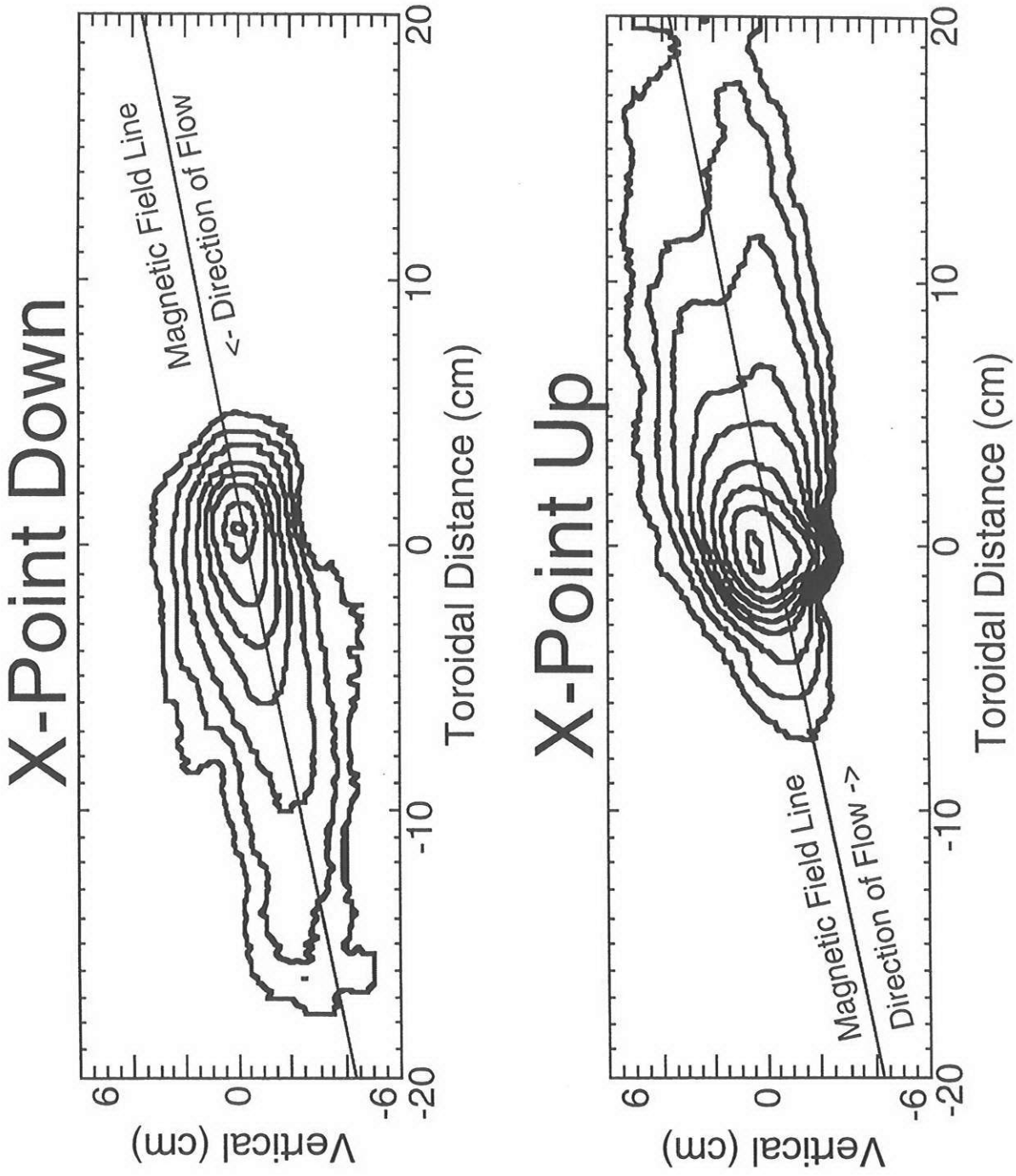
X-Point Down
Magnetic Field Line
<- Direction of Flow
Vertical (cm)
6
0
-6
-20
-10
0
10
20
Toroidal Distance (cm)
X-Point Up
Magnetic Field Line
Direction of Flow ->
Vertical (cm)
6
0
-6
-20
-10
0
10
20
Toroidal Distance (cm)

Figure 3

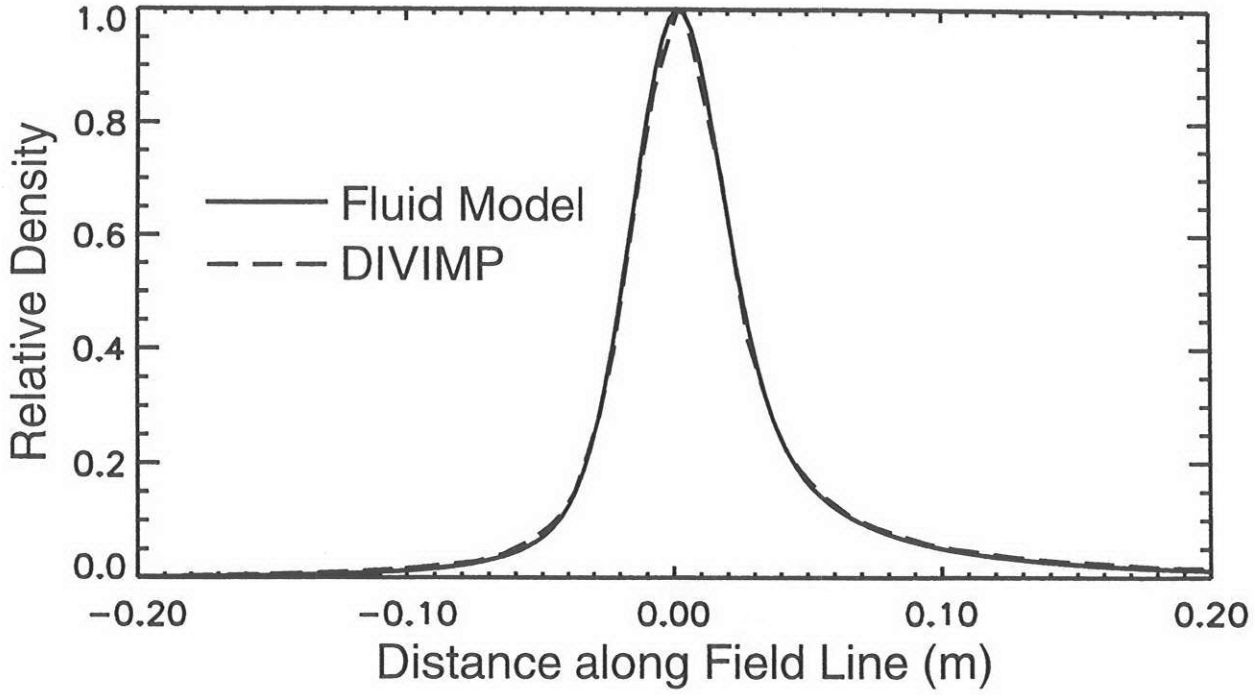
Relative Density
1.0
0.8
0.6
0.4
0.2
0.0
Fluid Model
DIVIMP
−0.20
−0.10
0.00
0.10
0.20
Distance along Field Line (m)

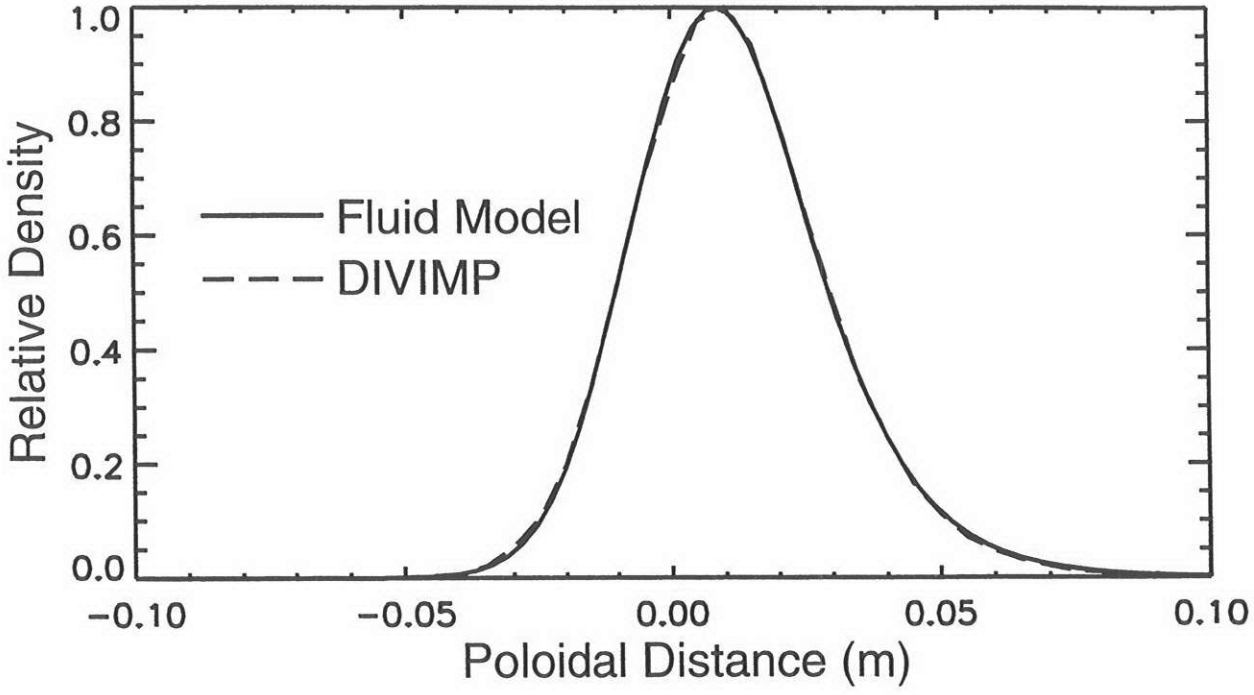
Relative Density
1.0
0.8
0.6
0.4
0.2
0.0
Fluid Model
DIVIMP
−0.10
−0.05
0.00
0.05
0.10
Poloidal Distance (m)

Figure 4

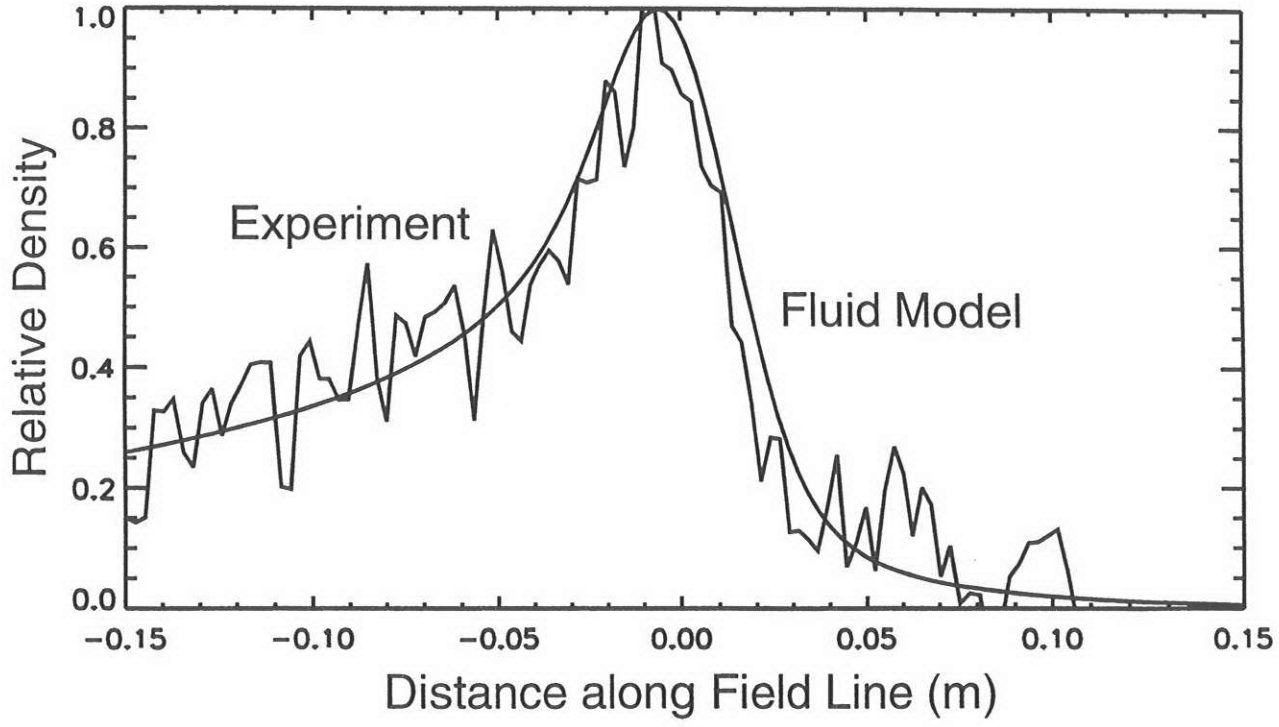
Relative Density
1.0
0.8
0.6
0.4
0.2
0.0
Experiment
Fluid Model
−0.15
−0.10
−0.05
0.00
0.05
0.10
0.15
Distance along Field Line (m)

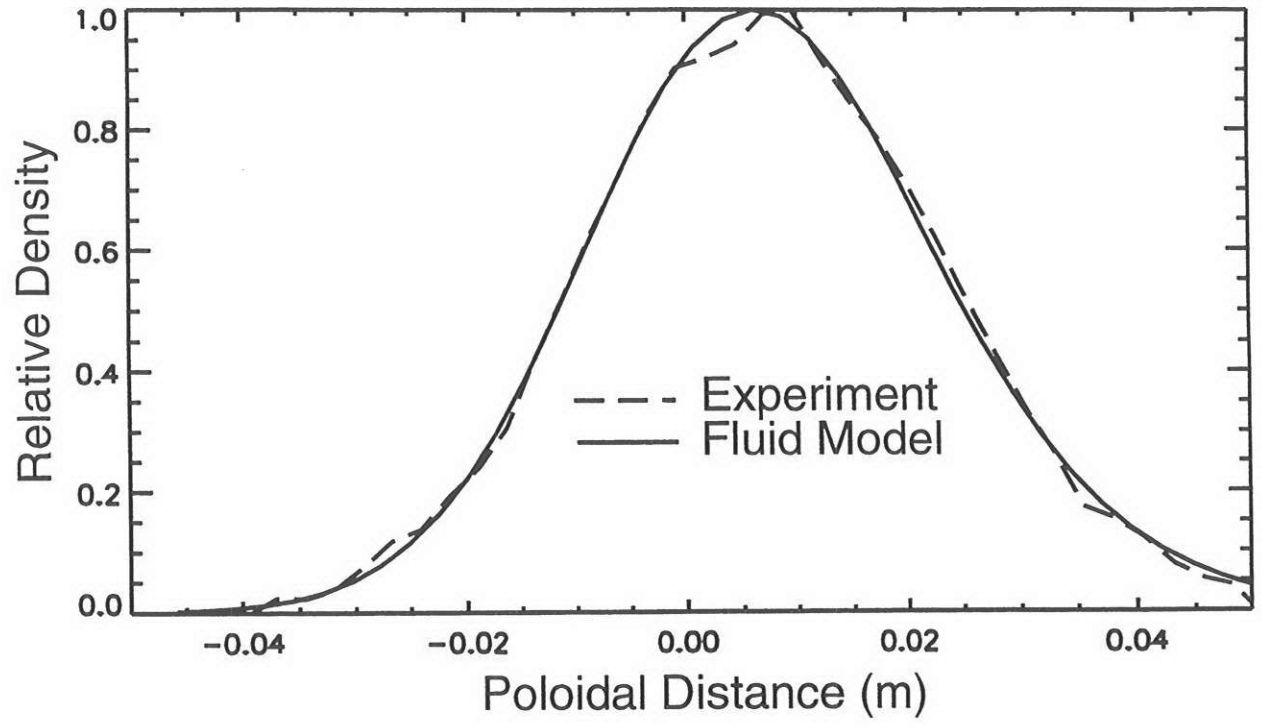
Relative Density
1.0
0.8
0.6
0.4
0.2
0.0
Experiment
Fluid Model
−0.04
−0.02
0.00
0.02
0.04
Poloidal Distance (m)

Figure 5